



Title	Synthesis of single- and multi-component carbides utilizing exfoliated graphite
Author(s)	Konno, Hidetaka; Abe, Daisuke; Habazaki, Hiroki
Citation	炭素, 2006(221), 8-13 https://doi.org/10.7209/tanso.2006.8
Issue Date	2006-01-16
Doc URL	http://hdl.handle.net/2115/72920
Rights	著作権は炭素材料学会にある。利用は著作権の範囲内に限られる
Type	article
File Information	tanso221-8.pdf



[Instructions for use](#)

Synthesis of single- and multi-component carbides utilizing exfoliated graphite

Hidetaka Konno[✦], Daisuke Abe and Hiroki Habazaki

Different metal alkoxides were impregnated into exfoliated graphite (EG) by sorption and hydrolyzed with steam. Thus formed precursors were pyrolyzed at 1500-1700 °C for 1-10 h in argon to form single- and multi-component carbides, such as ZrC, TiC, (Ti, Zr) C solid solutions, TiC-ZrC composites, and TiC-Fe composites. In this process, hydrolyzed metal alkoxides were converted mainly to oxides and/or oxyhydroxides on the surface of graphite sheet composing EG, and eventually they are reduced to carbide or metal by graphite carbon at elevated temperatures. The small reaction spaces in EG produce fine metal carbide particles only by the pyrolysis. The process is simple and low cost, and possible to be developed to synthesize other carbides and composites.

KEYWORDS: Exfoliated graphite, Metal alkoxide, Metal carbide, Multi-component carbide, Metal-carbide composite

1. Introduction

Metal carbides are industrially useful materials due to their unique characteristics. More than a few hundreds papers are published on the synthesis of metal carbides and composites by using elegant techniques, such as combustion synthesis, mechanical alloying, chemical method using alkaline or alkaline-earth metals as a reductant, laser abrasion, various vapor phase methods including application of plasma, and so on. Most of them, however, are not useful for mass production because of high cost, complicated processes, use of toxic and hazardous materials, low productivity, and so on. Accordingly, commercial processes to produce fine particles of carbides rely on the carbothermal reduction of metal compounds (mainly oxides) by carbon (mainly cokes), except for the production of extremely high purity powder. CVD processes are commonly used for that purpose.

We have reported a simple and low cost process to produce sub-micrometer-sized particles of β -SiC using exfoliated graphite (EG) and silicone¹⁾. The process does not require special instruments but uses only a high temperature furnace that can be run in inert atmosphere, and raw materials are inexpensive and not hazardous. The EG is known to have very high sorption capacity for oils^{2), 3)}, and the sorption capacity depends on the bulk density and the pore volume but not on the specific surface area³⁾. The sorption is caused by capillary action in the gaps of EG and the spaces created by entangled EG. Utilizing this property, precursors can be prepared by sorption of various organic liquids, such as the organic solutions

of metal complexes and organometallic compounds, metal alkoxides, silicone compounds, and so on, into EG. Heating these precursors in inert atmospheres produces a variety of carbon composites containing metals, metal oxides, and/or ceramics, and also carbides. The point of this process is that the precursor must be thermally stable to some extent, otherwise the materials impregnated in EG evaporate by heat treatment at elevated temperatures. In the present work, metal alkoxides were used as raw materials and they were converted to meta-stable states by hydrolysis in steam. Thus, ZrC, TiC, (Ti, Zr) C solid solutions, TiC-ZrC composites, and TiC-Fe composites were synthesized utilizing exfoliated graphite as reaction spaces and a reductant.

2. Experimental

2.1 Materials

Deliberately, reagents of low purity and low cost were used if available: they were zirconium (IV) tetra-n-butoxide (85 %, Kanto Chemical), titanium (IV) tetra-n-butoxide (97 %, Kanto Chemical), $\text{Fe}(\text{NO}_3)_3 \cdot 9\text{H}_2\text{O}$ (99 %, Kanto Chemical), and 1-butanol (99 %, Kanto Chemical). The EG was commercially available one produced from natural graphite of 130 μm in average diameter. The maximum sorption capacity of A-grade heavy oil was about 85 g/g, and a specific surface area 62 $\text{m}^2 \text{g}^{-1}$ ^{2), 3)}.

2.2 Preparation and pyrolysis of precursors

Prescribed amounts of reagents were dissolved into 1-butanol in which EG was added. The mass ratio of metal alkoxide and 1-butanol to EG was set to a value that does not exceed 30 g/g

[✦] Corresponding Author, E-mail: ko@eng.hokudai.ac.jp
Graduate School of Engineering, Hokkaido University: Sapporo 060-8628, Japan

(Received Sep. 6, 2005, Accepted Oct. 20, 2005)

considering the sorption ability of EG. Hereafter, precursor composition is referred to as $Zr/C = 0.39$, and so on, by mole ratio, where the amounts of carbon are only based on EG and those from organic functional groups of reagents are excluded. The sorption of the 1-butanol solutions by EG took place quickly. The formed composites were exposed in steam of the saturated vapor pressure at 60 or 80 °C for 1-3 h, and dried in a vacuum for 1.5 h. Hereafter, hydrolyzing temperature and time are denoted as T_h and t_h , respectively.

The precursors were pyrolyzed at a fixed temperature in a range of 500-1600 °C for 1-10 h in a flow of argon. Heating rate was 400 K h⁻¹ for 500-1200 °C and 300 K h⁻¹ for 1200-1600 °C due to different furnaces used.

2.3 Characterization of products

Conventional X-ray diffraction (XRD, Rigaku RAD-X RIND2000, Cu K α) measurements were carried out to estimate the composition of products. For the determination of lattice constants, precise XRD measurements were also done using 99.99 % pure silicone powder as an internal standard under the following conditions: Cu K α [$\lambda=0.15406$ nm] (40 kV, 25 mA), scanning step 0.02 deg [2 θ], counting time 5 s step⁻¹. The surface of products were directly observed by scanning electron microscopes (SEM, JEOL JSM-6300F at 3 kV, and JSM-6500F at 5 kV). Fine structure of Ti-Zr carbides was observed by a transmission electron microscope (TEM, JEOL JEM2010FX at 200 kV) and the composition was determined by energy dispersed X-ray analysis (EDX) under the same instrument. For TiC/Fe composites, elemental mapping was carried out by electron probe micro analysis (EPMA, JEOL JSM-5410-Oxford WDX400, at 20 kV). The TiC/Fe composites were attempted to dissolve with aqua regia but it was unsuccessful. Metal content was estimated by thermogravimetry up to 1000 °C at 10 K min⁻¹ in oxygen. The formed oxide was examined by XRD and metal content was calculated. The values, however, were used only as a measure of decomposition reactions, since some products were not converted to oxides completely under the above conditions.

3. Results and discussion

3.1 Synthesis of ZrC fine particles

In order to determine an appropriate mole ratio of Zr/C for precursor, different composites having $Zr/C = 0.11-0.45$ were prepared and hydrolyzed under the condition of $T_h = 60$ °C and $t_h = 3$ h. After drying, they were pyrolyzed at 1600 °C for 1 h. As shown in Fig.1, diffraction peaks of ZrC (JCPDS 35-784) are observed for all the products, but C 002 peak due to EG is also observed for the products from the precursor of $Zr/C \leq 0.34$ and the peaks of monoclinic ZrO₂ (JCPDS 37-1484) for the product from the precursor of $Zr/C = 0.45$. Accordingly, preferable Zr (IV)/C is around 0.39, and $Zr/C = 0.39$ was used hereafter, though a trace of C 002 peak appeared occasionally. The same results were

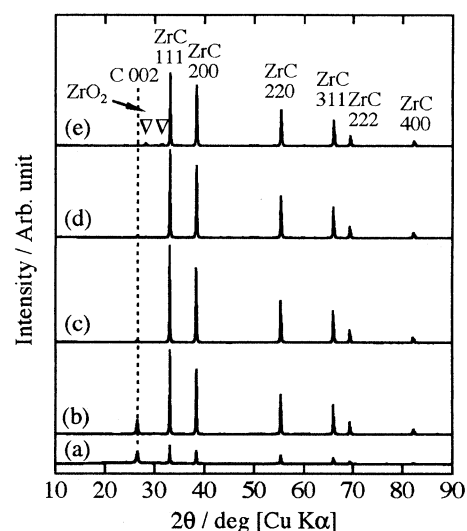


Fig.1 XRD patterns of the products formed by 1 h treatment at 1600 °C in argon from precursors of different compositions: $Zr/C =$ (a) 0.11, (b) 0.22, (c) 0.34, (d) 0.39, (e) 0.45 ($T_h = 60$ °C, $t_h = 3$ h).

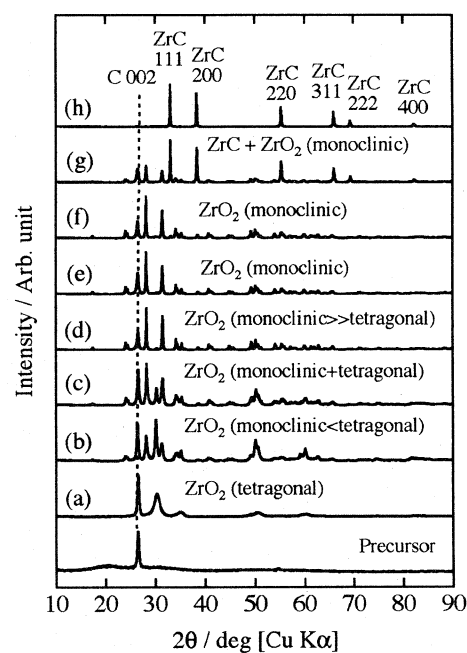


Fig.2 XRD patterns of the products formed by 1 h treatment at different temperatures of (a) 500 °C, (b) 1000 °C, (c) 1100 °C, (d) 1200 °C, (e) 1300 °C, (f) 1400 °C, (g) 1500 °C, and (h) 1600 °C. The precursor was $Zr/C = 0.39$ ($T_h = 60$ °C, $t_h = 2$ h).

obtained with $Zr/C = 0.39$ by $T_h = 60$ °C and $t_h = 2$ h, but when t_h was shorter than this, yield became very low.

Using the precursor of $Zr/C = 0.39$ and $t_h = 2$ h, decomposition scheme was followed by XRD, SEM, yield and Zr content, as shown in Figs.2, 3 and 4, respectively. Here, XRD patterns were measured after cooling the products to ambient temperature. The precursor does not show particular diffraction peaks except for those from EG (Fig.2) and the surface is something like the bed

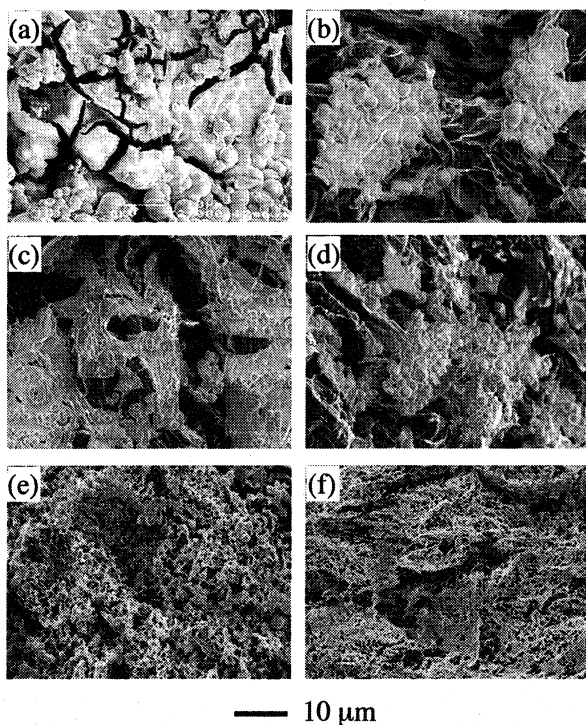


Fig.3 SEM images of (a) precursor (the same with Fig.2) and the products at different temperatures of (b) 500 °C, (c) 1000 °C, (d) 1400 °C, (e) 1500 °C, and (f) 1600 °C.

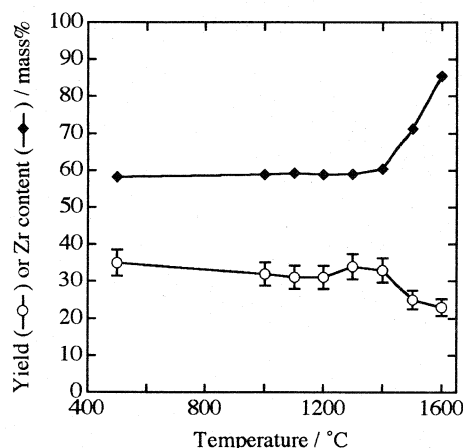


Fig.4 Temperature dependence of yield and Zr content for the products from the same precursor with Fig.2.

of dried up pond with many cracks (Fig.3 (a)). With increasing temperature of pyrolysis, the intensity of C 002 peak decreases (Fig.2 (a)-(g)) and the peak disappears by 1600 °C treatment (Fig.2 (h)). By 500 °C treatment, tetragonal ZrO₂ (JCPDS 42-1164) is formed (Fig.2 (a)) and eventually monoclinic ZrO₂ replaces the tetragonal type with increasing temperature, and up to 1400 °C no other by-products are observed by XRD. The Zr content of the products is constant up to 1400 °C and so as the yield, which is scattered a little due to experimental error (Fig.4). Hydrolyzed products covering EG become thin (less than 1 μm) and separate into ameba-like fragments with increasing temperature but such appearance is kept up to 1400 °C (Fig.3 (b)-(d)). Sharp diffraction

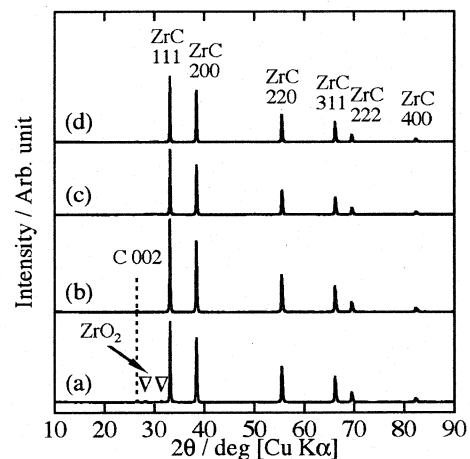


Fig.5 XRD patterns of different products, (a) pyrolysis: 1500 °C, 5 h; precursor: Zr/C = 0.39, $T_h = 60$ °C, $t_h = 2$ h, (b) pyrolysis: 1500 °C, 10 h; precursor: Zr/C = 0.39, $T_h = 60$ °C, $t_h = 2$ h, (c) pyrolysis: 1600 °C, 5 h; precursor: Zr/C = 0.39, $T_h = 80$ °C, $t_h = 2$ h, and (d) pyrolysis: 1600 °C, 1 h; precursor: Zr/C = 0.39, $T_h = 60$ °C, $t_h = 2$ h, ground.

peaks of ZrC appears from 1500 °C (Fig.2 (g) and (h)) and simultaneously Zr content increases and yield decreases (Fig.4). It is evident from Fig.3 (e) and (f) that EG disappears around 1500 °C and ZrC is formed as particles of sub-micrometers in size.

From the above results, it is reasonably concluded that Zr(IV) oxides (and oxyhydroxides) are formed from the hydrolyzed products of zirconium (IV) tetra-n-butoxide at as low temperature as 500 °C and they are converted to ZrC by EG above 1400 °C, namely by carbothermal reduction. However, there may be additional schemes of carbide formation by considering the results with precursors hydrolyzed at higher temperature and the formation of TiC described below. The formation of sub-micrometer-sized particles is probably owing to the reaction between very thin ameba-like fragments of ZrO₂ and EG. Formed ZrC is thin due to the shape of the precursors (Fig.3 (b)-(d)) and the reaction releases CO gas, leading to spontaneous formation of fine particles.

Additional experiments were carried out to improve the formation conditions and the products. First, prolonged pyrolysis was done at 1500 °C. As shown in Fig.5 (a) trace amounts of ZrO₂ remain by 5 h treatment but it disappears after 10 h (Fig.5 (b)). Lattice parameter was $a = 0.4681$ nm, and according to the Vegard's rule the product was ZrC_{0.82}O_{0.18} using $a = 0.46930$ nm for ZrC (JCPDS 35-784) and $a = 0.46258$ nm for ZrO (JCPDS 51-1149). This is comparable to the average composition of the product by 1 h treatment at 1600 °C, though the champion data under this condition is $a = 0.4692$ nm (ZrC_{0.985}O_{0.015}). Calculated oxygen content was 2-3 mass % and similar to that of low grade commercial products. Second, by increasing T_h to 80 °C the final yield was raised to about 40 mass % which was much higher than 20-25 mass % in Fig.4. The by-products, however, were not eliminated by 1 h treatment at 1600 °C, and 5 h was required as shown in Fig.5 (c). This large

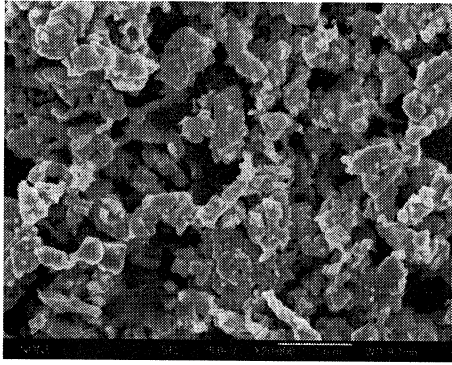


Fig.6 A SEM image of the product (d) in Fig.5.

increment of yield from the precursor having same Zr/C is possible only by taking into account spontaneous formation of carbide without EG. Third, for the formation of much finer particles, the precursor was ground with an agate mortar and pestle before pyrolysis. The product is perfectly single phase by XRD as shown in Fig.5 (d) and the particle size is a few hundreds nanometers as shown in Fig.6.

3.2 Synthesis of TiC fine particles

The survey experiments were carried out by changing the mole ratio, Ti/C, of precursor from 0.35 to 0.39 (hydrolysis: $T_h = 80^\circ\text{C}$ and $t_h = 2$ h) and the condition of pyrolysis from 1600°C , 1 h to 1700°C , 1 h. Again Ti/C = 0.39 was preferable but by 1 h treatment at 1600°C a trace of C 002 and TiO_2 (rutile) peaks remained occasionally, as shown in Fig.7 (f). Accordingly, 5 h treatment at 1600°C is necessary to form single phase TiC (by XRD) as shown in Fig.7 (g). This result is similar to the formation of ZrC from the precursor by $T_h = 80^\circ\text{C}$ described above. Two points may be considered to explain this. There were much more macroscopic cracks in the hydrolyzed products covering EG by $T_h = 80^\circ\text{C}$ than by $T_h = 60^\circ\text{C}$ (cf. Fig.3 (a)), which suggests that the hydrolyzed products are not very plastic, and oxides (and oxyhydroxides) formed at higher T_h may agglomerate more densely. With lower T_h some alkoxides and/or fragments from alkoxide may remain in the precursor and they will sublime during the pyrolysis, leading to the formation of flaws in the covering layers. The former is unfavorable and the latter is favorable to the reaction between the covering products and EG.

The formation scheme of TiC is similar to that of ZrC from XRD pattern of the products (Fig.7) and yield and Ti content (Fig.8), but some of the results are not readily understood. Yield decreases steeply from 1000°C to 1200°C , but Ti content does not increase substantially. TiC starts to form from much lower temperature than ZrC (Fig.2). It is clear from XRD pattern and Ti content that TiC is formed above 1200°C , but the yield at 1300°C is practically the same with those of 1100 - 1200°C . On synthesizing β -SiC from EG and silicon, EG did not function as a reductant below 1500°C ¹⁾. As shown in Fig.3 (d), graphite sheet of EG remained at 1400°C and so was the case of TiC formation process, though SEM images

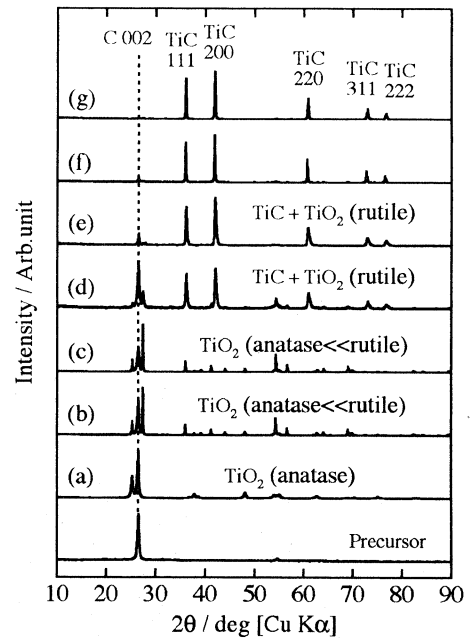


Fig.7 XRD patterns of the products formed by 1 h treatment at different temperatures of (a) 500°C , (b) 1000°C , (c) 1200°C , (d) 1300°C , (e) 1500°C , (f) 1600°C , and (g) 5 h treatment at 1600°C . The precursor was Ti/C = 0.39 ($T_h = 80^\circ\text{C}$, $t_h = 2$ h).

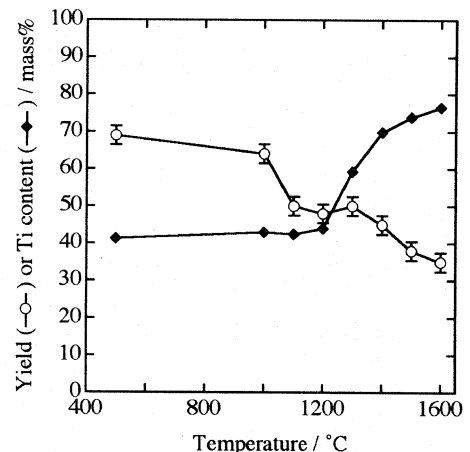


Fig.8 Temperature dependence of yield and Ti content for the products from the same precursor with Fig.7.

were omitted. These results strongly suggest that TiC formed at 1300°C (Fig.7 (d)) is not ascribed to carbothermal reduction by EG. There is a possibility that the inconsistencies observed in Fig.8 have occurred by chance owing to different processes superposed. In sum, TiC is formed from TiO_2 , which is the main decomposition product of precursor, by the reaction with EG, but considerable amounts are also formed by the pyrolysis of precursor alone. The formation of ZrC should be considered similarly.

The average lattice parameter was $a = 0.4303$ nm, and according to the Vegard's rule the product was $\text{TiC}_{0.84}\text{O}_{0.16}$ using $a = 0.43274$ nm for TiC (JCPDS 32-1383) and $a = 0.4177$ nm for TiO (JCPDS 8-117), but the results is not accurate, since a reliable a value for TiO of S.G. Fm3m is not available. The products were fine particles

of sub-micrometers in size similar to ZrC in Fig.6.

3.3 Synthesis of (Ti, Zr)C solid solutions and TiC-ZrC composites

As ZrC and TiC are soluble each other, (Ti, Zr)C solid solutions were attempted to synthesize. According to a phase diagram⁴⁾, calculated solubility of ZrC to TiC is lower than about 9 mol % and that of TiC to ZrC is lower than about 27 mol % at 1600 °C. Based on the results of single component carbides, synthesis has been started using a precursor of $(\text{Ti}_{0.5}\text{Zr}_{0.5})/\text{C} = 0.39$ (hydrolysis: $T_h = 60\text{ °C}$ and $t_h = 2\text{ h}$) but with this mole ratio by-products were not eliminated. For the present, preferable conditions were found as follows: Precursor: $(\text{Ti} + \text{Zr})/\text{C} = 0.45$ (hydrolysis: $T_h = 80\text{ °C}$ and $t_h = 2\text{ h}$); pyrolysis: 1600 °C, 5 h. The XRD patterns of products from the precursors of various Ti/Zr mole ratios are shown in Fig.9. As expected from the phase diagram, solid solutions were formed with the precursors of $\text{Ti}/\text{Zr} = 96/4$ and $\text{Ti}/\text{Zr} \leq 21/79$. With $\text{Ti}/\text{Zr} = 67/33$ and $50/50$, TiC-ZrC composites were formed, and ZrO_2 was not eliminated with the latter composition. Actually, very weak diffraction peaks of TiC are observable in the solid solutions of $\text{Ti}/\text{Zr} \leq 21/79$, so that there may be more suitable conditions to synthesize these solid solutions.

A TEM image and the results of EDX analysis of the product from the precursor with $\text{Ti}/\text{Zr} = 50/50$ are shown in Fig.10. The EDX spectrum numbers are corresponding to the particles in the TEM image and Cu peaks are due to a holder mesh. The electron beam size was about 20 nm, so that the EDX spectrum represents the composition of each particle. As oxygen is not detected in particle 2, it is TiC based solid solution with ZrC. In particle 4, however, an

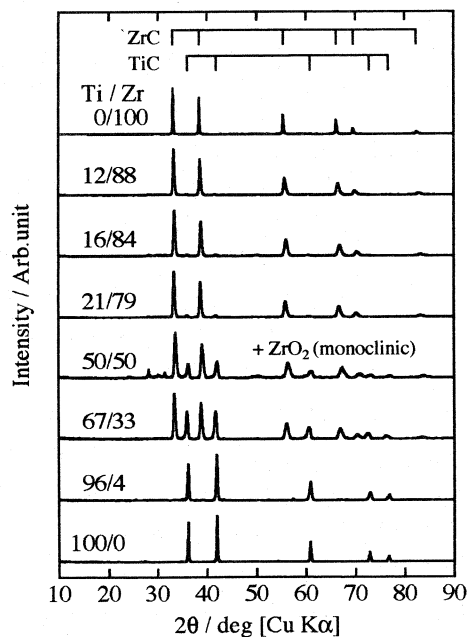


Fig.9 XRD patterns of the products formed by 5 h treatment at 1600 °C from precursors of different Ti/Zr mole ratios. The precursor was $(\text{Ti} + \text{Zr})/\text{C} = 0.45$ ($T_h = 80\text{ °C}$, $t_h = 2\text{ h}$).

oxygen peak is larger than a carbon peak, so that it may be ZrO_2 detected by XRD (Fig.9). In any particles both Ti and Zr are detected, indicating that the product is not a composite of single phase TiC and ZrC, but composed of solid solutions close to the end-compositions. The results indicate that the quality is different for each particle, and so there is ample room for further improvement of the precursor and pyrolysis condition. The TEM image indicates that the formed particles are smaller than 200 nm. It is a distinctive feature of the present process that sub-micrometer-sized fine particles are produced only by pyrolysis of much larger precursors.

3.4 Synthesis of TiC-Fe composites

Formation of TiC-Fe composites was attempted, since it has been studied for providing one of the potential alternatives to WC-Co composites⁵⁾⁻⁷⁾. The precursor was prepared based on the one for TiC ($\text{Ti}/\text{C} = 0.39$; hydrolysis: $T_h = 80\text{ °C}$ and $t_h = 2\text{ h}$) with adding iron (III) nitrate to be $\text{Fe}/\text{Ti} = 0.1-1.0$ in mole ratio. Only for this system, the final drying was done in a vacuum oven at 110 °C for 1.5 h, because of water carried by iron (III) nitrate.

Initially, pyrolysis was carried out at 1600 °C for 5 h after the example of TiC synthesis. It provided composites of TiC and α -Fe

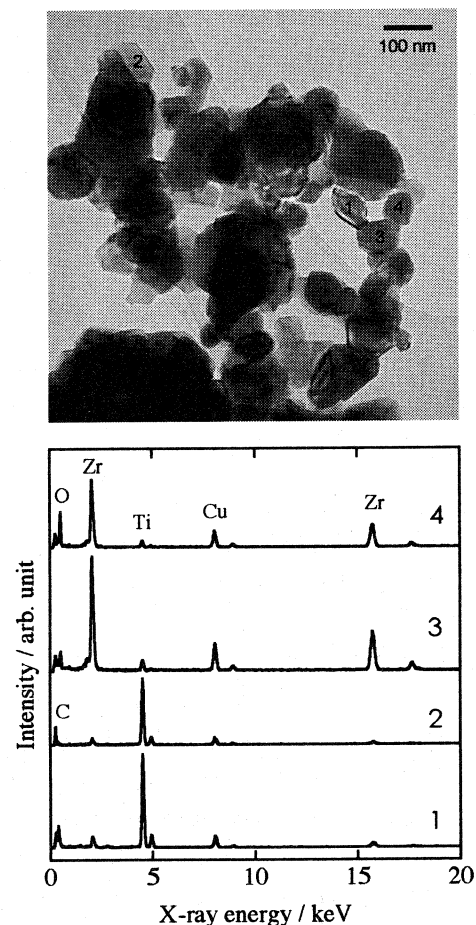


Fig.10 A TEM image (upper) and the results of EDX analysis (lower) of the products from the precursor of $\text{Ti}:\text{Zr} = 50/50$ in Fig.9. The numbers in the lower figure correspond to analyzed particles in the upper image.

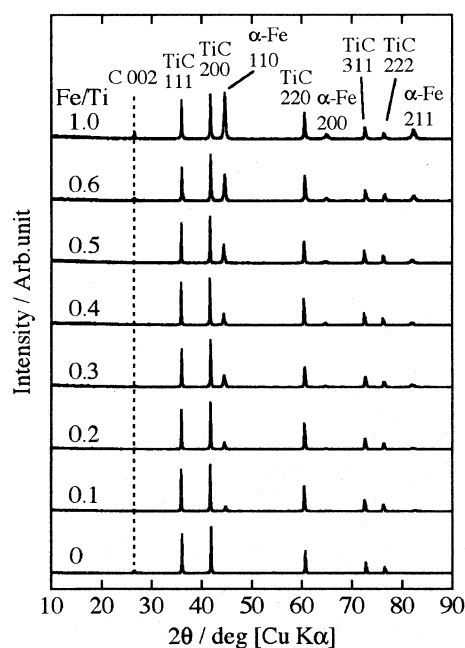


Fig.11 XRD patterns of the products formed by 1 h treatment at 1600 °C from precursors of different Fe/Ti mole ratios. The precursor was Fe added Ti/C = 0.39 ($T_h = 80$ °C, $t_h = 2$ h).

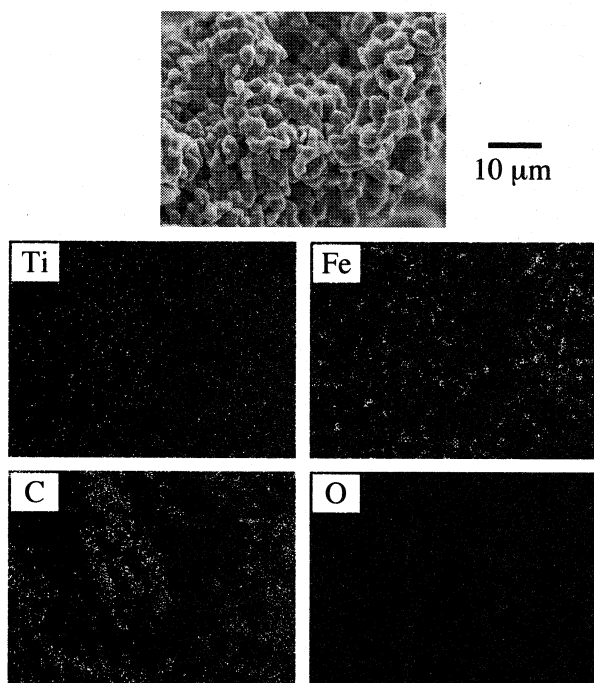


Fig.12 A SEM image of the product form the precursor of Fe/Ti = 0.3 in Fig.11 and its elemental mapping by EPMA.

at any composition ratios, though small diffraction peak of C 002 due to EG was distinguished when Fe/Ti \geq 0.4. For Fe/Ti \geq 0.3 TiC particles embedded in α -Fe was observed by EPMA, but the particle size became as large as 10 μ m, especially for larger Fe/Ti products. To inhibit growth of TiC particles, pyrolysis time was shortened to 1 h. The XRD patterns of the products are shown in Fig.11. This condition is not suitable to form single phase TiC (by XRD) as shown in Fig.7 (f), but when Fe (III) was added to

the precursor, by-products were not observed, except for EG. Naturally, intensity of α -Fe diffraction peaks increases with increasing Fe/Ti. Even under this condition, some TiC particles grew up to about 10 μ m, when Fe/Ti \geq 0.6. In Fig.12, a SEM image and elemental mapping images by EPMA for the product from the precursor of Fe/Ti = 0.3 are shown. Elemental mapping images are distorted due to the rough sample surface, but it is seen that particle size is a few micrometers and TiC particles are surrounded by α -Fe. The intensity of oxygen is much lower than that of carbon; the relative intensity of oxygen was apparently lower than the case of TiC described in 3.2, though the data by EPMA were omitted there. The results indicate that composites of TiC and α -Fe is possible to be produced by the present process.

Summary

As described above, single metal carbides, multi-component metal carbides, and carbide-metal composites are possible to be synthesized, using the precursors prepared from metal-alkoxides and exfoliated graphite (EG). Metal-alkoxides are easily taken by sorption into the spaces or gaps between thin graphite sheets, which construct the frame structure of EG. Thin layers of intermediate compounds formed by hydrolysis and subsequent heat-treatment are eventually converted to carbides in the small reaction spaces of EG, leading to the formation of fine metal carbide particles only by pyrolysis. The main reaction scheme is carbothermal reduction of oxides by EG at elevated temperatures, but the formation of carbides by spontaneous decomposition of intermediate compounds at a little lower temperatures is also contributing. Some amounts of dissolved oxygen are present in the products, and so the process must be improved more, but the present process can be developed to synthesize other carbides and composites. and is promising for industrial applications.

Acknowledgment

This work was partly supported by the Grant-in-Aid for Scientific Research (B) (No.13450279) from JSPS and the Ookura Kazuchika Memorial Foundation.

References

- 1) H. Konno, T. Kinomura, H. Habazaki and M. Aramata, *Carbon* **42** (2004) 737-744.
- 2) M. Toyoda and M. Inagaki, *Carbon* **38** (2000) 199-210.
- 3) M. Toyoda, K. Moriya, J. Aizawa, H. Konno and M. Inagaki, *Desalination* **128** (2000) 205-211.
- 4) *Phase Equilibria Diagrams*, Vol.X (1994) p.368, The American Ceramic Society.
- 5) Y. Choi and S. W. Rhee, *J. Mater. Res.* **8** (1993) 3202-3209.
- 6) P. Persson, A. E. W. Jarfors and S. Savage, *J. Mater. Proc. Tech.* **127** (2002) 131-139.
- 7) I. W. M. Brown and W. R. Owers, *Curr. Appl. Phys.* **4** (2004) 171-174.